Guidelines for the construction of a generating partition in the standard map

Freddy Christiansen [a], Antonio Politi [b],*

[a] The Max Planck Institute for Complex Systems, Dresden, Germany
[b] Istituto Nazionale di Ottica, INFN. Sezione di Firenze, I-50125 Firenze, Italy

Abstract

The validity of a recently developed procedure to construct a symbolic dynamics for the standard map is accurately investigated. The implications of all the stages, that involve the determination of homoclinic tangencies and the identification of appropriate symmetry lines, are discussed. Moreover, an extension of the method from the strongly to the weakly chaotic regime is presented. As a result, the general validity of the approach is strengthened, although many intermediate steps still have no rigorous justification.

1. Introduction

The development of general methods to construct generating partitions (GPs) is of primary importance to reach a detailed understanding of the evolution of dynamical systems. The task appears to be particularly difficult in conservative systems since both the chaotic and the quasiperiodic motion must be simultaneously accounted for. A very promising approach has been recently proposed in [1] with reference to the standard map in a highly chaotic regime. It combines the concept of homoclinic tangencies (HTs) – a key ingredient for the encoding of chaotic motion in dissipative systems [2] – with the notion of symmetry lines [1] which allow the description of quasiperiodic motion. Although any kind of symmetry can be exploited in the construction of a GP, it is worth stressing here that it is the invariance under time reversal

that plays the prominent role in the whole process, so that we may safely state that the method has a broad range of applicability (no peculiar feature of the standard map has been, indeed, used in [1]). However, the success of the implementation depends on several conditions and conjectures that are neither rigorously proved nor widely numerically tested. For instance, it has not been proved that the procedure to construct a GP can be pushed to an arbitrary degree of accuracy. Moreover, the concept of primary homoclinic tangency (PHT), so important in the identification of a GP, has not been formalized yet and, in numerical applications, one is unable to ascertain whether a given point is a homoclinic tangency at all.

An important open question is also why HTs and symmetry lines can be coherently combined within a single consistent approach: it is, for instance, unexplained why the symmetry lines pass through the "bifurcation" points where two lines of HTs collapse together, thus allowing the construction of a continuous partition border.

* Corresponding author.
[1] See Section 2 for a definition of symmetry line.

Another point requiring a deeper understanding concerns the connection between chaotic and quasiperiodic regions. It is well known that within any stability island exists an infinite hierarchy of higher-order islands. Accordingly, an infinite hierarchy of increasingly thinner chaotic layers is present as well, which must be properly encoded. Again, we can only state that the "experimental" procedure fulfills all the properties that are a priori required down to the accuracy that has been possible to reach. Although there are no explanations of the above-mentioned points, the observations made for different parameter values induce us to conjecture the general validity of the underlying ideas.

Insofar as the main justification for the whole method comes from the "experimental" evidence of its functioning, it is of a particular relevance to test its validity in various models and for various parameters. For this reason, in Section 2, we furnish a critical exposition of the method, with reference to the standard map, but in a sufficiently general language so as to clarify the role of all the relevant intermediate

steps. We hope that this presentation, together with a new effective algorithm recently proposed for the identification of HTs [3], will contribute to facilitate future investigations. Anyway, we can already register that a first confirmation of the goodness of those ideas has already come from their application in the context of the analysis of hydrogen in a magnetic field [4].

In Section 3 we investigate again the standard map, but in a very different regime, the weakly chaotic behavior occurring at small nonlinearities. In fact, this problem is not obviously related to the previous one. The quasiperiodic motion is the main component to start the construction of a GP. Nevertheless, we shall find unexpected similarities that reinforce the feeling that the validity of this encoding technique follows from very general arguments.

2. Highly chaotic regime

The standard map is a general prototype for the study of low-dimensional Hamiltonian chaos which arises in several contexts. We adopt the following representation for the equations of motion:

$$
\begin{aligned}
x_{n+1} &= y_n \\
y_{n+1} &= -x_n + 2y_n - \alpha \cos(y_n) \bmod 2\pi,
\end{aligned}
\tag{1}
$$

since it offers a more natural description of the underlying folding process. We shall sometime use the shorthand notation $\mathbf{X}_{n+1} = F(\mathbf{X}_n)$. There are two relevant symmetries in the dynamics of map (1): (i) the invariance under time reversal expressed by the equality $T \circ F \circ T = F^{-1}$, where T is the involution $T(x, y) = (y, x)$; (ii) the invariance under the transformation $S(x, y) = (\pi - x, \pi - y) \bmod 2\pi$, i.e., $F = S \circ F \circ S$.

The discussion on the construction of the GP starts from the observation that the phase-space, being a torus, has no natural boundaries, so that one must include the task of tiling the plane with equivalent elementary cells. In [5], it has been shown that one of the lines around which the phase-space is folded (plus its backward iterate) is perfectly suited for this aim (see Fig. 1 where the line of interest is L_2). Accordingly, the problem of constructing a GP is reduced to that
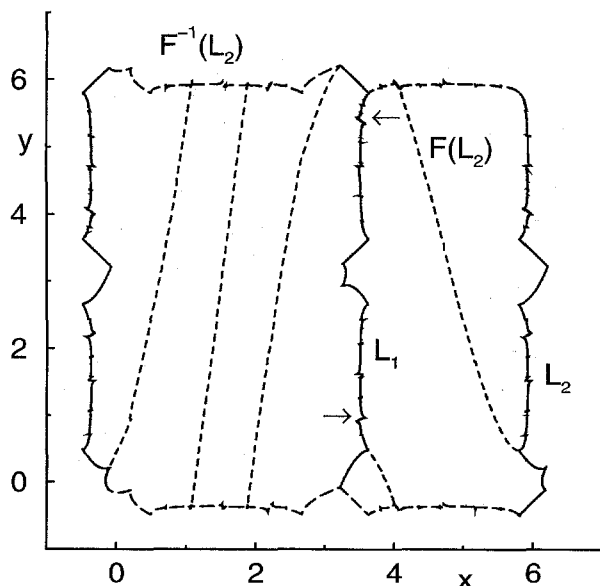

Fig. 1. Generating partition in the standard map for $\alpha = 6$. The borderline of the partition is made of primary HTs bridged by symmetry lines. The two arrows point to a pair of conjugated avoided crossings.

of identifying such "folding" lines. The sine function entering the definition of the standard map implies the presence of two distinct folding lines. Since they are related by the S-symmetry, one is obtained from the other by applying the transformation S. Therefore, from now on we restrict our analysis to just one of them.

A folding line is a curve separating two regions of the phase-space that, since they are eventually squeezed against each other, must be encoded with different symbols. In the highly chaotic regime, a folding line is approximately given by the set of points where the first iterate of a vertical line is bent, i.e., the vertical line $x = \sin^{-1}(-2/\alpha)$. In Fig. 1, one can notice that for $\alpha = 6$, this line is indeed very close to the curve L_1 eventually obtained through the more rigorous procedure discussed below. The starting point consists in recognizing that a folding point is nothing but a homoclinic tangency, since the curvature of the unstable manifold around the forward iterates of each HT diverges asymptotically. Moreover, since any (either forward or backward) iterate of a HT is a tangency itself, HTs can be thought of as arranged in distinct doubly infinite sequences of points. It is obvious that only a single tangency within each sequence is truly needed to discriminate among trajectories lying on opposite sides of the folding line. This leads to the problem of singling out the most suitable point, the *primary* tangency, within each sequence of HTs. Although this step has not yet been rigorously formalized, in general, the idea of considering the tangencies which lie approximately in the folding regions turns out to represent a good starting point. The main problems that one has to face arise whenever a piece of a HT line is mapped onto another such piece, since lines of homoclinic tangencies always give rise to avoided crossings. This phenomenon is precisely a consequence of the fact that a folding region is mapped again along the folding line after a finite number of iterates, leading to an exchange between stable and unstable directions. One such example is the zone indicated by the upper arrow in Fig. 1, which is mapped in two iterates in the region indicated by the lower arrow. A closer look at the alignment of HTs can be given in Fig. 2,
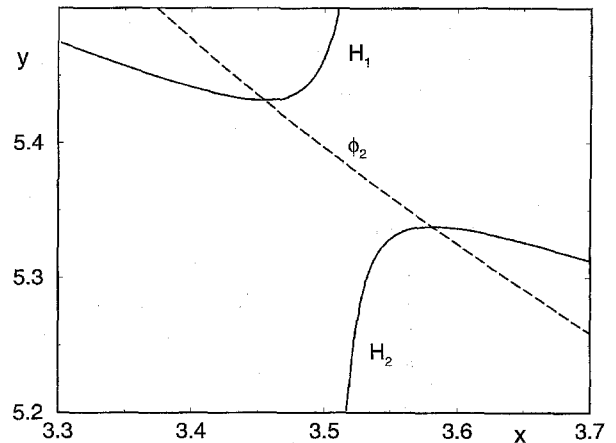

Fig. 2. Enlargement of the region indicated by the upper arrow in Fig. 1. The solid lines refer to the sequences of homoclinic tangencies which, first approach and then move away from one another, giving rise to a typical avoided crossing. The dashed curve indicates the symmetry lines used to bridge the gap.

where a magnification of the region of interest is reported.

The presence of avoided crossings imply that other concepts should be invoked to enable a connection of the disjoint branches of tangencies into a continuous line. A convincing solution to this problem has been proposed in [1], where it was suggested to use symmetry lines. Let us here present a two-step general argument supporting such a conjecture. The first step starts from the observation that we could have proceeded equally well in the construction of the GP by looking for the folding points along the stable, rather along the unstable manifold. Because of the invariance of the dynamics under time reversal, we would have obtained just $T(L_1)$. Now, since a HT is a HT independently of whether we look at forward or backward iterates, the line $T(L_1)$ should differ from L_1 only for it being some forward or backward iterate of it. This is indeed the case for the standard map, where it is found that

$$L_1 = F(T(L_1)). \tag{2}$$

While the above equality is automatically satisfied by the HTs, it plays the role of a constraint for the lines that could be used to connect the HTs with a single continuous line.

However, Eq. (2) alone is not enough to identify such lines. It is no more than a symmetry condition, expressing how different sections of L_1 are mutually related. This problem is solved with the second step of our argument, which starts from the observation that avoided crossings (the places where the additional lines are to be placed) occur in pairs,[2] since they arise when a given section R_0 of L_1 is mapped onto another section R_n of L_1 after n iterates, i.e. $R_n = F^n(R_0)$.

The two observations can now be put together to find a unique solution, by noticing that the elements of a given pair (R_0, R_n) are also connected by the above-mentioned time-reversal symmetry, so that we can write down the relation

$$F^n(x, y) = F \circ T(x, y). \qquad (3)$$

Therefore, the curves are parts of the set of fixed points for the mapping

$$\phi_n(x, y) = T \circ F^{n-1}(x, y), \qquad (4)$$

which turns out to be an involution, since

$$\phi_n \circ \phi_n = T \circ F^{n-1} \circ T \circ F^{n-1}$$
$$= T \circ T \circ F^{1-n} \circ F^{n-1}$$
$$= \mathrm{id},$$
$$\det \frac{\mathrm{d}\phi_n(x, y)}{\mathrm{d}(x, y)} = -1. \qquad (5)$$

The set of fixed points is called a symmetry line ϕ_n [6]. The symmetry line bridging the gap in Fig. 2 is ϕ_2, $x = y - (\alpha/2) \cos y \bmod \pi$ (see the dashed curve). Accordingly, the partition border can be constructed by connecting the branch of HTs denoted with H_1 in the figure first with ϕ_2 and then with H_2. This construction is perfectly self-consistent since the HTs in that do not contribute to the partition border are indeed (second) preimages of primary tangencies used to define the borderline in the region indicated by the lower arrow in Fig. 1 [1].

The existence of the further symmetry S implies the existence of gaps which are connected by this transformation. They can be treated in a similar way by invoking the corresponding set of symmetry lines. Two important observations are in order. First, the length of the segments of symmetry lines needed to bridge the various gaps decrease very rapidly to zero for $n \to \infty$, so that the line L_1 eventually obtained, though nowhere differentiable, does not appear to be too wild. Second, the symmetry lines turn out to intercept the sequence of HTs precisely in the "bifurcation" points where a PHT collapses with a secondary tangency [1]. This is an important coincidence that allows passing from one (HTs) to another (symmetry lines) ingredient precisely where the first one can no longer be used.

The last problem in the construction of a GP in the strongly chaotic regime concerns stability islands, that are typically present also in this case. A general, though non-universal, solution can again be obtained with the aid of symmetry lines. Let us first observe that the quasiperiodic motion occurring within a stability island can be properly encoded by monitoring the rotation angle around the center O of the island, if the frequency varies with the distance from O.[3] The rotation can, in principle, be quantified by splitting the island into two complementary sectors through the introduction of suitable semi-axes departing from the center O. The symbol sequence is then obtained by associating a different symbol to each sector.

Now, from the very definition (4) of symmetry line, it can be straightforwardly verified that an orbit of period N which is invariant under time reversal, lies at least along two such curves ϕ_n for $-N \geq n \leq N$. Accordingly, the two lines match the above-mentioned properties for a meaningful encoding of the quasiperiodic motion. However, while, on the one hand, there are infinitely many symmetry lines passing through O, on the other hand, there is, a priori, no guarantee that any such line leads to a meaningful representation not only of the motion within the primary island but also inside the secondary and higher-order islands.

It is an "experimental" observation that there always exists (at least) a symmetry line passing through the centers of all the secondary islands, which can thus be successfully used to encode not only the rotation around O but also the rotation occurring around the

---

[2] The only exceptions are when a given region is mapped back onto itself. This case is not, however, conceptually different.

[3] The degeneracy occurring in the harmonic oscillator is truly exceptional.

secondary centers. Although such a line does not suffice to encode tertiary islands as well, a preliminary analysis reveals that higher-order symmetry lines can be effectively used to further refine the partition border. It is therefore reasonable to conjecture that the whole procedure can be iterated all the way down to infinitesimal scales.

A further problem concerns the thin chaotic layers separating the various islands. A detailed numerical analysis of this question is very difficult because of the extremely weak and slow folding process. We shall see in Section 3 that they can be consistently included into the global procedure.

The last comment regards the nature of the islands. They have been so far assumed to be invariant under time reversal. Whenever this is not true, the whole construction does not apply: evidently, symmetry lines do not pass through asymmetric solutions. In this case, we can only say that other types of arguments should be introduced. We consider this as the only truly open problem. However, in favor of the procedure so far described, we can say that this difficulty does not affect the validity of all the other steps and, moreover, it implies only the lack of a well-defined criterion to choose the borderline of the partition. Experimentally, though, we have observed that the secondary centers of asymmetric islands do line up along smooth curves and we can thus hope that they can be treated in a similar way to symmetric islands. Furthermore, we have observed, upon varying α, that asymmetric islands play a very marginal role in that they exist only in very tiny intervals compared to those of the symmetric ones.

3. Weakly chaotic regime

In this section, we study the standard map for small values of the nonlinearity, when most of the phase space is filled with quasiperiodic orbits. Therefore, it does not make much sense to start the construction of the partition border from the identification of the folding regions. This is clearly confirmed by the first iterate of a generic vertical line which is not bended anywhere (i.e. the equation $\sin x = -2/\alpha$ has no solution).
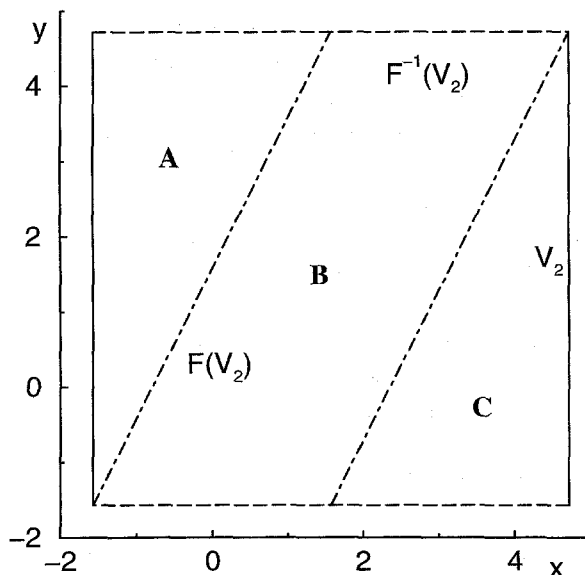
Fig. 3. Partition for $\alpha = 0$. The various lines split the square into three regions encoded with the symbols A, B, and C, respectively.

It is, instead, instructive to consider first the limit case $\alpha = 0$ in which the phase-space is foliated by the invariant tori $y - x = \beta$ with $\beta \in (-\pi, \pi)$. In this case, it is obviously impossible to construct a rigorously "generating" partition, since for any rational β, there is a continuum of periodic orbits all characterized by the same rotation angle. On the one hand, this difficulty can be safely disregarded, as it occurs only in a perfectly integrable dynamical system, such as the standard map for $\alpha = 0$. On the other hand, we expect that a meaningful partition should nevertheless be able to discriminate among orbits corresponding to different rotation angles, because this is a feature that will survive after switching on the nonlinearity. The simplest way to encode the rotations is achieved by defining the elementary cell as a square with the lower-left corner in the point $(\bar{x}, \bar{x})$, for an arbitrary $\bar{x}$. A symbolic dynamics can then be constructed by adding the bisectrix $y = x$ which splits the elementary square cell into two triangular sectors. If we associate the symbol $b = 0$ to the upper triangle and $b = 1$ to the lower one, it is immediately realized that the motion along the line $y_n = x_n + \beta$ is encoded in the same way as free rotation in the circle map.

An alternative partition, which has the advantage of not requiring new ingredients besides the borders of the elementary cell, is obtained by replacing the bisectrix with the image of a vertical edge of the square. As a result, the phase-space is split in three rather than two regions (see Fig. 3 for the assignment of the symbols $s = A$, B, and C). The new representation can be obtained from the previous one, by the following rules: $s_n = B$ whenever the pair $b_{n-1}b_n$ is either 00 or 11; $s_n = A$ ($s_n = C$) if $b_{n-1}b_n = 10$ ($b_{n-1}b_n = 01$). Conversely, $s_n = A$, C implies $b_n = 0$, 1, while C is translated into either 0 or 1, depending on the value of the last non-C observed in the past: an A implies that $b_n = 0$, while a B implies that $b_n = 1$.

Although the latter partition is clearly redundant, we prefer to stick to it, since it is closer, in spirit, to the partition introduced in Section 2 and thus it allows a more direct comparison of the symbolic dynamics in the two limits.

Let us now discuss the new features that arise when the nonlinearity is switched on. First of all, it is an "experimental" observation that all the primary stability islands are aligned along the vertical line V_2, $x = 3\pi/2$. This is still true for $\alpha = 0.9$, as it can be seen in Fig. 4 where all periodic orbits up to length 10 have been reported together with the largest chaotic component (some of the periodic orbits along V_2 are unstable since they have already undergone a period doubling bifurcation). As a consequence, V_2 is the line to be used as the right border of the elementary cell (apart from higher-order adjustments), since it allows encoding the motion inside the islands. This is a very important feature, as it removes the ambiguity about the value of $\bar{x}$.

Before proceeding further on, let us summarize that, at this stage, the partition involves V_2 (and the same line shifted by 2π) and its forward and backward images as seen in Fig. 3. Accordingly, this is very much in the spirit of the strongly chaotic case, where L_2 was playing the role of V_2. The main qualitative difference between the two cases is that, here, we have no line such as L_1 to further split the phase space. Symmetry considerations provide a convincing explanation of this difference: while $L_1 = S(L_2)$, $V_2 = S(V_2)$, so that the two lines perfectly overlap in the present case!

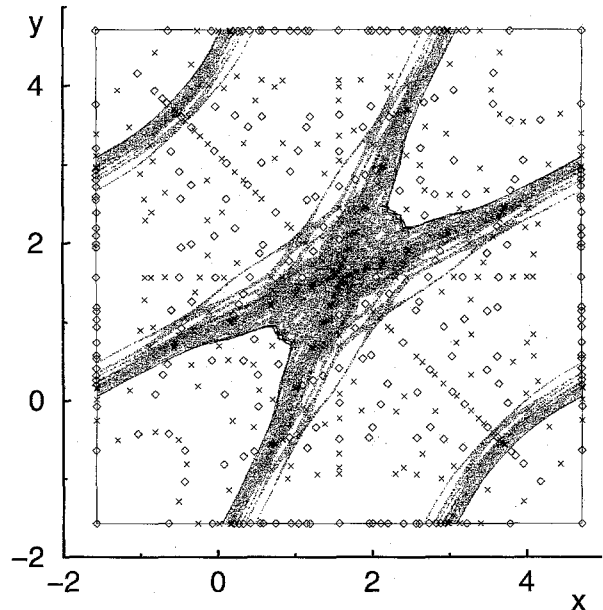

Fig. 4. The largest chaotic component and all periodic orbits up to period 10 for $\alpha = 0.9$. Diamonds denote stable orbits, while crosses refer to unstable ones.

It is instructive to notice that V_2 is invariant also under time reversal, i.e. $V_2 = F(T(V_2))$. This latter symmetry, shared also by L_2, is very important as it ensures the invariance of the symbolic dynamics under time reversal.

As in the strongly chaotic regime, the main task will now be the refinement of V_2 although, now we have to proceed in the opposite way, starting from symmetries and inserting HTs afterwards. First of all, the line V_2 should be refined every time it crosses a primary island (and the associated hierarchy of sub-islands). We illustrate the procedure with reference to the main island (centered around the fixed point $(3\pi/2, 3\pi/2)$). From the data reported in Fig. 5, one can see that it is the line $y = 3\pi - x$ that should be used to refine the partition inside the island, since it passes through the stable sub-chains as well. This is perfectly consistent with the previous investigation which suggested us to use the fixed points of the involution $F^{n-1}(x, y) = TS(x, y)$ to refine the partition inside an S-symmetric island of period-n. In the specific case of the period-1 island, $f^0 = TS$ gives the above-mentioned line. Incidentally, let us also notice that this is the same line
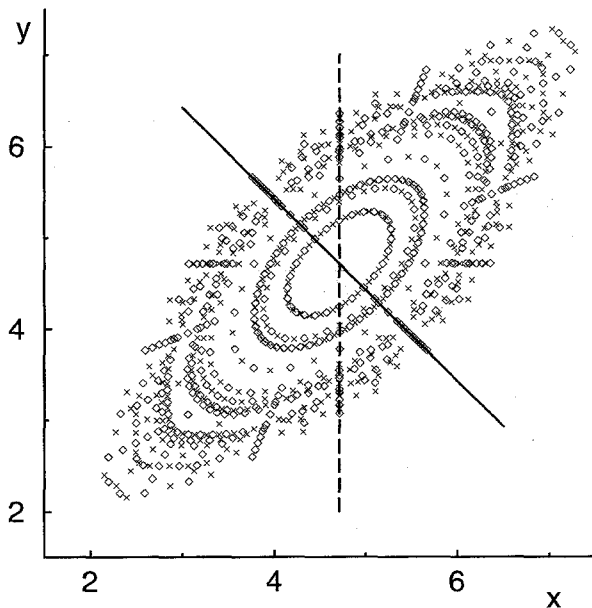
Fig. 5. Periodic orbits inside the main stability island for $\alpha = 0.9$. Diamonds and crosses refer to stable and unstable orbits, respectively. The dashed curve corresponds to the line $x = 3\pi/2$, while the solid curve corresponds to $y = 3\pi - x$. Notice that the latter one passes through stable orbits only.

Fig. 6. Some of the primary homoclinic tangencies inside the large chaotic component surrounding the main stability island for $\alpha = 0.9$. It is clearly seen that they are almost aligned along a virtual curve connecting the solid line, which acts as a partition border inside the island, with the dashed line, representing the border in the external quasiperiodic region.

Fig. 7. V_2 (solid line) and V_1 (dashed line) after the refinement to account for all stability islands up to period 5. Notice that y and x are here exchanged to prepare a picture with a more convenient aspect ratio.

used for the period-2 island present for $\alpha = 6$. This is a nice correspondence, since the period-2 island is the result of period doubling of this fixed point and, therefore, it represents a further indication of the generality of the whole procedure.

The use of symmetry lines does not exhaust the construction of a continuous partition line: in the vicinity of each resonance, we need to connect the line $x = 3\pi/2$, which acts as a border out of the island, with the symmetry line used inside the island. We conjecture that this connection should consist of HTs. In Fig. 6, we have plotted part of the main island and of the corresponding chaotic layer together with a set of HTs determined with the technique introduced in [3]. HTs appear to lie precisely in the region where they can effectively be used to bridge the gap between different symmetry lines. A more accurate construction of this partition border would require the approximate identification of the folding line to be used as a reference for defining the primary tangencies as it was done in the strongly chaotic case. However, the weakness of
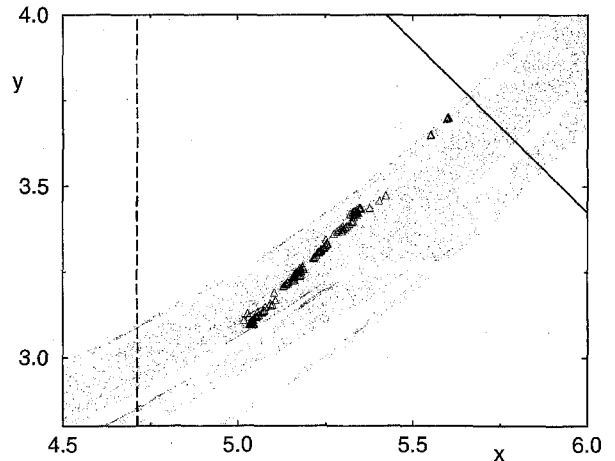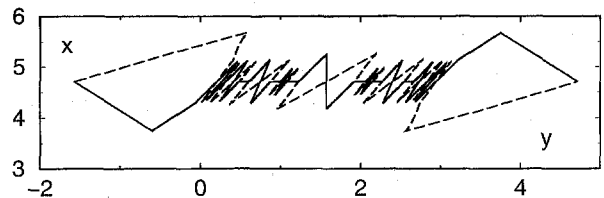
the chaotic process requires a very delicate numerical investigation that goes beyond the scope of the present paper. We leave to a future work, as well as the inclusion of the islands existing inside the chaotic sea. Here, we limit ourselves to observe that, coherently with the analysis developed in Section 2, the line of HTs points towards the bigger islands.

The partition can be refined in a similar way inside all the other primary islands. The corrections arising from handling period 2–5 orbits are reported in Fig. 7, where rather strong transversal oscillations can be observed. They suggest that V_2 might eventually become a fractal curve with an infinite length; we leave this

point to a future investigation. Moreover, let us mention that besides stability islands, there are, obviously, KAM tori (as long as they survive). For their encoding, it is still true what has been stressed at the very beginning of this section: any vertical line works equally well. For consistency reasons with the rest of the islands, we have decided to choose $x = 3\pi/2$ also in this case.

The partition could be obtained by adding to the refined V_2 both its forward and backward image. However, again symmetry considerations reveal a weak point of the resulting encoding. While all the adjustments introduced along V_2 automatically maintain its invariance under the S-transformation, the same is not true for the FT-symmetry, which is violated. In fact, after the refinement, $F(T(V_2)) \neq V_2$. Accordingly, the symbolic encoding does not preserve the time-reversal symmetry of the original model. A simple way to restore the symmetry is by adding the line $V_1 = F(T(V_2))$ as a further partition border. Both V_1 and V_2 are reported in Fig. 7, where it can be seen that they differ only inside each stability island where two symmetric triangular blobs are opened (all islands up to period 5 are considered). If we then use V_1 in the same way as L_1 was considered in Section 2, we finally obtain the partition that is reported in Fig. 8. Since V_2 represents the border line of the elementary cell, every time V_1 lies to the left, a blob originates in the right part of the cell (see the black regions in the figure), while the opposite occurs whenever V_1 is to the right of V_2. Although the various blobs seem to be disconnected from one another, we must keep in mind that an infinitely accurate refinement would lead to infinitely many blobs with point-like connections. We conjecture that they can be attributed the same symbol and this is confirmed by a direct numerical implementation of the partition. Through the following below of what happens to the GP at the period doubling bifurcation of a stable orbit, we shall see that this idea is less bizarre than it could appear.

To underscore the connection between the construction of the GPs for the two different regimes, we want to give a flavor of how the GP changes when α is increased. We limit ourselves to illustrate the process with reference to the main stability island, all the
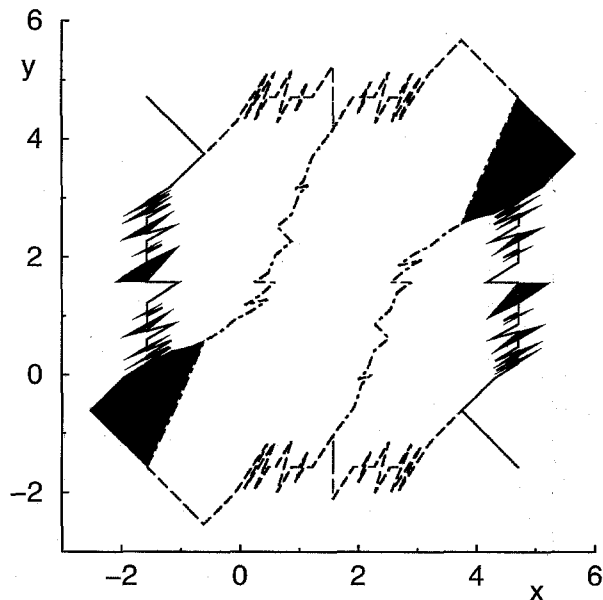

Fig. 8. The resulting partition at $\alpha = 0.9$. The regions colored in black denote the set delimited by V_1 and V_2, which requires an additional symbol with respect to the limit case $\alpha = 0$.

others giving rise to a similar picture. Inside the island, the two partition lines V_2 and V_1 are given (in a first approximation) by the straight line $x + y = \pi$, and its symmetric $F(T(V_2))$, independently of α (as long as the fixed point remains an elliptic one). This can, for instance, be noticed in Fig. 9(a), where the structure of the island with the two symmetry lines is reported for $\alpha = 3.7$. The partition borders can still be constructed in a similar way to the above discussed case $\alpha = 0.9$. Upon changing α, V_1 turns clockwise until it becomes tangential to V_2 at the fixed point for $\alpha = 4$. This is the moment when period doubling occurs, giving rise to the period-2 islands that are still present at $\alpha = 6$. After period doubling, the two border lines of the partition are constructed in a different way, since the fixed point is now hyperbolic and there is no need for a border line to pass through it. It becomes, instead, necessary to include those segments that pass through the period-2 orbit. As a result, the two partition lines turn out to pass through the two points of the same period-2 orbit, respectively. Accordingly, they do not cross each other anymore (see Fig. 9(b) for the new construction) and, as a consequence, a curious
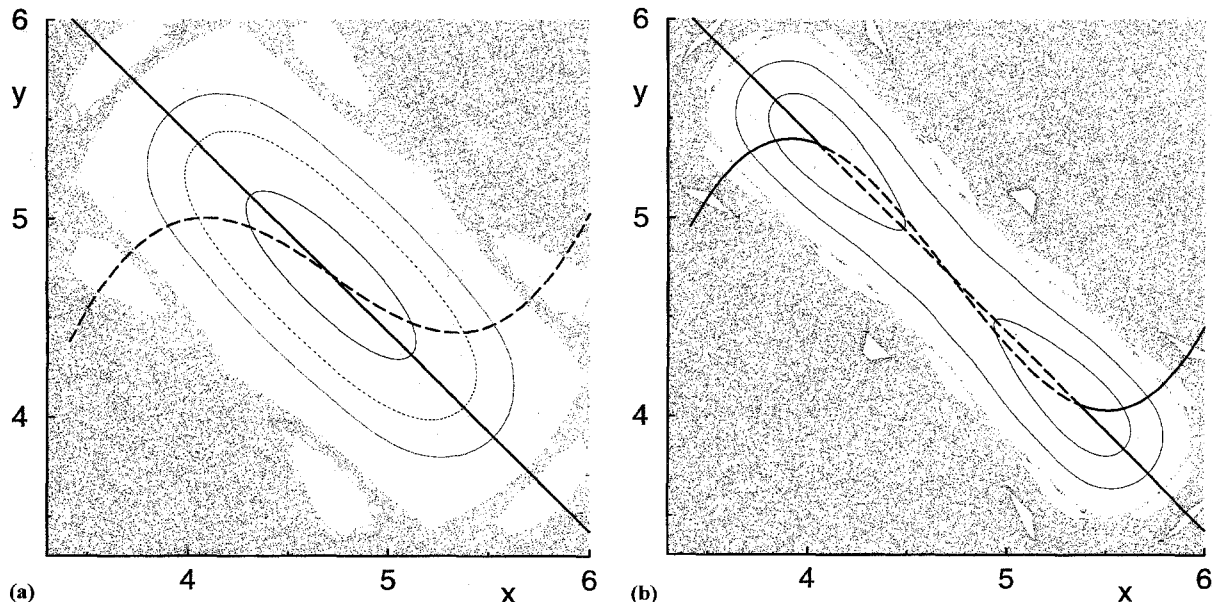
Fig. 9. A picture of the main island around its period-doubling. (a) $\alpha = 3.7$, when the fixed point is still elliptic; the solid curve denotes the symmetry line $y = 3\pi - x$, while the dashed curve is its $F \cdot T$ image. Both serve as partition borders. (b) $\alpha = 4.3$, when a stable period-2 orbit is generated. The partition borders are now represented by the two solid lines which are completely separated from one another.

exchange of symmetry occurs: instead of having two lines such as V_1 and V_2 which are separately S-symmetric but non-invariant under time reversal, we find two lines like L_1 and L_2 which are separately invariant under time reversal, but no longer S-symmetric.

4. Conclusions

In this paper, we have shown that the procedure developed in [1] for the construction of a GP in the strongly chaotic regime of the standard map can be successfully extended to the weakly chaotic case. Although many steps still deserve a detailed analysis and a rigorous justification, the method appears to work and, moreover, interesting similarities have been detected between the two opposite limits. A careful scrutiny of these relationships is certainly necessary in order to shed further light on the whole procedure, but this represents the subject of a future research project. In particular, we want to stress that whether

the partition introduced in this paper can be simplified is an open question. More precisely, we expect that it should be possible to eliminate some redundancy (let us, for instance, recall the partition involving only two symbols that is able to account for the dynamics in the limit case $\alpha = 0$). It is not, however, clear whether this can be accomplished without destroying the similarity with the strongly chaotic regime.

Acknowledgements

Both authors wish to acknowledge the editors of this special volume for their patience in waiting for the completion of the manuscript.

References

[1] F. Christiansen and A. Politi, Nonlinearity 9 (1996) 1623.
[2] P. Grassberger and H. Kantz, Phys. Lett. A 113 (1995) 235.

[3] L. Jaeger and H. Kantz, Homoclinic tangencies and non-normal Jacobians – the effects of noise in non-hyperbolic dynamical systems, Physica D, in press.

[4] K. Hansen and S. Güttler, Symbolic dynamics for hydrogen in a magnetic field, J. Phys., to be submitted.

[5] F. Christiansen and A. Politi, Phys. Rev. E 51 (1995) 3811.

[6] P.H. Richter, H.-J. Scholz and A. Wittek, Nonlinearity 3 (1990) 45.